

Nonlinear Orbital Variations in Binary Radio Pulsars from Lense-Thirring Precession

Emmanuel Fonseca*

*Department of Physics and Astronomy, West Virginia University,
PO Box 6315, Morgantown, WV 26506, USA and
Center for Gravitational Waves and Cosmology, West Virginia University,
Chestnut Ridge Research Building, Morgantown, WV 26505, USA*

(Dated: December 2, 2025)

A future measurement of Lense-Thirring (LT) precession using a binary radio pulsar is expected to yield the pulsar’s moment of inertia (I_p). However, most of the known pulsar-binary systems expected to provide this opportunity will exhibit linear variations in the orbital elements due to LT precession that are difficult to separate from variations induced by other mechanisms. In this work, we demonstrate that the pulsar-timing signature of LT precession for an arbitrary orbital orientation produces nonlinear orbital variations; if detected, these nonlinear variations provide a means to constrain I_p without the need for timing-independent measurements of orbital geometry or distance. We show through simulations that these signatures are indeed detectable in pulsar-binary systems with an appropriate combination of timing precision and orbital geometry. Our simulations also show that nonlinear orbital variations from LT precession are expected to be detectable in PSR J1757–1854 after only 15 yr of dedicated timing.

I. INTRODUCTION

Radio pulsars are spinning neutron stars that emit beamed radiation and are observed as pulses with clock-like regularity. This rotational stability is due to their large moments of inertia (I_p), with $O(I_p) \sim 10^{45} \text{ g cm}^2$. In the context of gravitational physics, pulsars serve as tools with a dual purpose: to test the validity of viable theories of strong-field gravitation, such as general relativity (GR); and to derive intrinsic properties of an orbital system and its constituents in accordance with the assumed theory [1]. Binary radio pulsars are regularly used to resolve “post-Keplerian” (PK) deviations from Newtonian orbital motion [2]; and by assuming that GR is correct, these PK measurements allow grant access to the gravitational masses of the observed pulsars (m_p) and their binary companions (m_c) with high precision [e.g., 3]. The most ideal systems for testing and utilizing GR are isolated “double-neutron-star” (DNS) binary systems, due to the point-like gravitational interactions between their constituent neutron stars.

Long-term timing measurements of DNS pulsars are expected to provide the first strong-field measurement of Lense-Thirring (LT) precession – the gravitoelectromagnetic precession of the orbital angular momentum vector \mathbf{L} about the total angular momentum vector \mathbf{J} due to the spin of the observed pulsar. The varying sense of \mathbf{L} due to LT precession will manifest as PK variations of the binary orientation angles – the inclination angle relative to the plane of the sky (i), the argument of periastrion (ω), and the longitude of the ascending node (Ω ; [4]). The future measurement of LT precession is highly anticipated as it will allow for a direct measurement of I_p and thus provide timing-based information on the equation of state (EoS) of neutron stars [e.g., 5].

Recent works have treated the expected pulsar-timing signature of LT precession as a secular (i.e., constant, first-order) PK variation in one or more orbital elements. However, the sense of both \mathbf{L} and the pulsar’s spin angular momentum vector \mathbf{S}_p evolve over time and in a periodic manner.[6] Therefore, LT precession can induce nonlinear variations in the orbital geometry if a sufficient amount of precession has occurred. In this work, we explore the efficacy in detecting nonlinear variations due to LT precession through pulsar timing. This work shows that sufficiently relativistic DNS systems can exhibit nonlinearity in orbital evolution due to LT precession over $O(10 \text{ yr})$, allowing for a timing-only derivation of I_p and the relevant spin-orbit orientation.

II. VARIATIONS FROM LT PRECESSION

Variations of the measurable Keplerian elements consist of terms intrinsic and extrinsic to the binary system [e.g., 7]. For example, timing modulations associated with orbital motion are proportional to the semi-major axis of the pulsar’s orbit (a_p) projected onto an observer’s line of sight, typically written as $x_{\text{int}} = a_p \sin i / c$ where c is the speed of light. In addition to inclination, the *observed* amplitude (x) is further modulated by two factors: a factor D quantifying the Doppler shift between an observer and the center of mass of a moving binary system; and a factor ϵ_p arising from special-relativistic aberration of the pulsed radio signal. The observed $x \equiv x_{\text{obs}} = D^{-1}(1 + \epsilon_p)x_{\text{int}}$. For the case of x , a variation in any of the relevant elements and/or (D , ϵ_p) similarly produces a variation that can be written as

$$\left(\frac{\dot{x}}{x}\right)_{\text{obs}} = -\left(\frac{\dot{D}}{D}\right) + \left(\frac{\dot{a}_p}{a_p}\right) + \cot i \left(\frac{\dot{di}}{dt}\right) + \frac{d\epsilon_p}{dt}. \quad (1)$$

The first and second terms of Equation 1 are known to

* emmanuel.fonseca@mail.wvu.edu

arise from relative acceleration in the Milky Way Galaxy [e.g., 8] and PK energy loss due to gravitational radiation [9], respectively. We treat these two contributions as constant as they vary on timescales much larger than those of existing data sets. By contrast, LT precession of \mathbf{L} about \mathbf{J} is expected to yield a PK variation in i which, in accordance with GR, corresponds to a rate

$$\left(\frac{di}{dt}\right)_{\text{LT}}^{\text{GR}} = \frac{2\pi G}{P_s c^2 a^3 (1-e^2)^{3/2}} \left(2 + \frac{3}{2} \frac{m_c}{m_p}\right) I_p \sin \lambda \cos \eta, \quad (2)$$

where G is Newton’s gravitational constant, P_s is the pulsar’s spin period, a is the semi-major axis of the relative orbit, e is the orbital eccentricity, and (λ, η) are the polar angles that define the sense of \mathbf{S}_p relative to the plane of the sky [10].

The fourth term arises from the varying aberration and is given by

$$\frac{d\epsilon_p}{dt} = -\frac{P_s}{P_b} \frac{\Omega_p}{\sin^2 \lambda (1-e^2)^{1/2}} (\cos \lambda \sin 2\eta + \cot i \sin \lambda \cos \eta), \quad (3)$$

where Ω_p is the rate of de Sitter (or “geodetic”) precession of \mathbf{S}_p about \mathbf{J} . Geodetic precession leads to non-linear rates of change in (λ, η) . The time dependence of (λ, η) therefore requires that Equation 2 – and thus $\dot{x}_{\text{LT}} = x \cot i (di/dt)_{\text{LT}}^{\text{GR}}$ – also depend on time. This time dependence can be written as a set of coupled trigonometric equations [7]:

$$\cos \lambda = \cos \delta \cos i - \sin \delta \sin i \cos(\Omega_p t + \Phi_0) \quad (4)$$

$$\cos \eta = \sin \delta \sin(\Omega_p t + \Phi_0) / \sin \lambda, \quad (5)$$

where $\delta = \cos^{-1}(\hat{\mathbf{L}} \cdot \hat{\mathbf{S}}_p)$ is the misalignment angle between the senses of \mathbf{L} and \mathbf{S}_p – labeled with the “hat” notation to indicate their respective unit vectors – and Φ_0 is a phase of orientation during the precession cycle.

The observed apsidal motion in pulsar-binary systems ($\dot{\omega} \equiv d\omega/dt$, where ω is the argument of periastron) is also expected to consist of additive terms associated with different mechanisms. For example, in the presently considered case of an isolated binary system, $\dot{\omega}_{\text{obs}} = \dot{\omega}_{\text{int}} + \dot{\omega}_{\mu} + \dot{\omega}_{\text{LT}}$, where $\dot{\omega}_{\text{int}}$ is the “intrinsic” term associated with relativistic point-particle dynamics [10], while $\dot{\omega}_{\mu}$ is an “extrinsic” bias due to proper motion of the binary system [11]. However, unlike \dot{x}_{LT} , $\dot{\omega}_{\text{LT}}$ is bilinear in $\hat{\mathbf{L}} \cdot \hat{\mathbf{S}}_p = \cos \delta$, which is constant, and $\hat{\mathbf{L}} \cdot \hat{\mathbf{K}} = \cos \lambda$, which itself consists of constant and time-variable terms as shown in Equation 4 [10]. This circumstance therefore means that $\dot{\omega}_{\text{LT}}$ consists of constant and time-variable components, i.e., $\dot{\omega}_{\text{LT}} = \dot{\omega}_{\text{LT},0} + \dot{\omega}_{\text{LT},t}$, where

$$\dot{\omega}_{\text{LT},0} = -\frac{4\pi G I_p \cos \delta}{P_s c^2 a^3 (1-e^2)^{3/2}} \left(2 + \frac{3}{2} \frac{m_c}{m_p}\right), \quad (6)$$

$$\dot{\omega}_{\text{LT},t} = +\frac{2\pi G I_p \cot i \sin \delta}{P_s c^2 a^3 (1-e^2)^{3/2}} \left(2 + \frac{3}{2} \frac{m_c}{m_p}\right) \cos(\Omega_p t + \Phi_0). \quad (7)$$

The observed effect can finally be written as $\dot{\omega} \equiv \dot{\omega}_c + \dot{\omega}_{\text{LT},t}$, where $\dot{\omega}_c = \dot{\omega}_{\text{int}} + \dot{\omega}_{\mu} + \dot{\omega}_{\text{LT},0}$ is the sum of constant terms.

Equations 2–7 demonstrate that the amplitudes of \dot{x}_{LT} and $\dot{\omega}_{\text{LT}}$ are proportional to I_p and various trigonometric factors of the orientation angles (i, δ, Φ_0) . The inclination i is calculable from the other observed GR effects under the assumption that GR describes all observed variations; this circumstance means that (I_p, δ, Φ_0) are the only *a priori* unknown quantities. In practice, (δ, Φ_0) can be constrained through the analysis of variations in “pulse structure” [7]. These methods primarily consist of modeling pulse-component broadening [12] as well as spin-resolved polarization evolution [13], both of which arising from geodetic precession. However, such efforts naturally introduce model dependency, e.g., a specific magnetic field structure to explain complex polarization variations [e.g., 14].

DNS systems with $i \approx \pi/2$ and/or $\delta \approx 0$ will yield $\dot{x}_{\text{LT}} \approx 0$ and $\dot{\omega}_{\text{LT}} \approx \dot{\omega}_{\text{LT},0}$, leaving I_p as the only unknown since $\cos \delta \approx 1$. However, the isolation of $\dot{\omega}_{\text{LT},0}$ from other terms requires the use of other well-measured relativistic effects to determine (m_p, m_c) for computing $\dot{\omega}_{\text{int}}$ accurate to second post-Newtonian (PN) order. In practice, such an effort will also require significant, independent measurement of other geometric parameters like the system distance to account for relative acceleration bias in observed orbital decay. This circumstance describes the ongoing effort to measure I_p for PSR J0737–3039A [15].

By contrast, DNS systems with lower inclination and $\delta > 0^\circ$ will exhibit $d\epsilon_p/dt$, \dot{x}_{LT} , and $\dot{\omega}_{\text{LT},t}$ over time. The detection of these terms and their time variability, if achievable, can therefore serve as direct constraints on (I_p, δ, Φ_0) obtained purely through pulsar timing. Robust estimates of all these quantities through timing variations from LT precession will nonetheless require specific observing conditions; these conditions can be assessed through simulations.

III. SIMULATIONS

We used the open-source PINT software suite [16], designed for pulsar-timing experiments, in order to assess the measurability of nonlinear variations from LT precession. We extended the existing “DDGR” binary timing model to include (a) second-PN-order corrections to all relativistic variations wherever relevant, and (b) Equations 2–7 into the parameterized expressions for \dot{x} and $\dot{\omega}$.

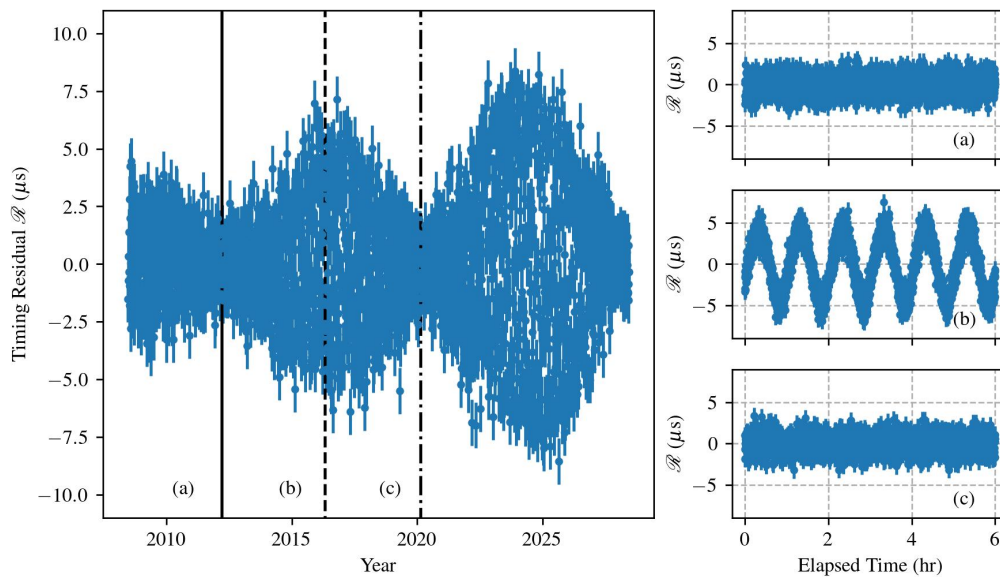


FIG. 1. Simulated pulsar-timing “residuals” of a fictitious binary pulsar, described in §III, that exhibits only the $\dot{\omega}_{LT,t}$ component of LT precession. The left panel shows residuals over a 20-yr timespan. The three smaller panels on the right show residuals evaluated over 6-hr time intervals, showing that timing effects from $\dot{\omega}_{LT,t}$ vary significantly for this hypothetical binary pulsar.

The resultant model therefore includes (I_p, δ, Φ_0) as degrees of freedom, along with the five Keplerian elements and (m_c, m_{tot}) .

For the purposes of simulation, we first considered an “idealized” pulsar-binary system with $P_b = 1$ hr, $a_p = 0.81$ lt-s, $e = 0.1$, $\delta = 10^\circ$, and $m_c = m_p = 1.4 M_\odot$. The value of a_p was chosen to ensure that $\cot i \sim 0.1$ as required by the Keplerian mass function. We assume that the idealized pulsar is sufficiently bright such that its arrival-time estimates yield a mean uncertainty of $1 \mu\text{s}$ after coherently averaging pulses acquired over 30-s intervals. This high timing precision is achievable in long-term timing studies of several known DNS systems.

Figure 1 shows the difference in simulated pulsar times of arrival (TOAs) between a timing model where $I_p = 1.25 \times 10^{45}$ g cm² and another where $I_p = 0$ g cm²; the latter model corresponds to a model where the timing effects from LT precession are ignored. For the purposes of illustration, Figure 1 shows TOA variations that arise only from $\dot{\omega}_{LT,t}$ alone and neglect the larger TOA perturbations from \dot{x}_{LT} and $d\epsilon_p/dt$. It is clear from Figure 1 that such an idealized pulsar will indeed exhibit nonlinear TOA variations due to the time-dependent component of $\dot{\omega}_{LT}$ by itself.

A detection of nonlinear orbital variations in either \dot{x} or $\dot{\omega}$ can be used to obtain timing-based estimates of terms involving combinations of (I_p, δ, Φ_0) . For example, a constraint on the amplitude of $\dot{\omega}_{LT,t}$ alone immediately yields a constraint on $I_p \sin \delta$; this circumstance will remain valid even if $\dot{\omega}_\mu$ is statistically significant, as $\dot{\omega}_\mu$ arises only as a constant, secular variation and therefore only impacts a separate measurement of $\dot{\omega}_{LT,0}$. Further-

more, a meaningful constraint on Φ_0 will become possible if the observing timespan T is a significant fraction of the precession cycle, i.e., $T \sim 2\pi/\Omega_p$. A detection of $d\epsilon_p/dt$ will only serve to constrain (δ, Φ_0) as it does not depend on I_p . In the absence of external information, measurements of all nonlinear variations – $d\epsilon_p/dt$, \dot{x}_{LT} , and $\dot{\omega}_{LT,t}$ – can allow for separate measurement of (I_p, δ, Φ_0) .

Our pulsar-timing simulation nonetheless required the union of unprecedented orbital compactness and high timing precision to yield successful detections of the nonlinear variations. Forecasts of the DNS population within the Milky Way Galaxy indicate that systems resembling the ideal system used for our simulations likely exist in modest numbers. However, it remains to be observed whether such ultra-compact DNS systems contain at least one pulsar that offers the required timing properties. Moreover, the population of known DNS pulsars exhibits a diverse range of compactness, timing precision, and orbital geometries. It is therefore worthwhile to determine if any of the known DNS pulsars will exhibit nonlinear orbital variations, whether in existing or forthcoming data sets.

IV. KNOWN BINARY PULSARS

The population of known DNS systems within the Milky Way Galaxy that contain at least one pulsar currently consists of $O(20)$ members. Nearly half of these systems yield one or more orbital variations due to GR and can therefore be considered “relativistic.” However, only a small fraction of these DNS pulsars have in-

PSR	m_p (M_\odot)	m_c (M_\odot)	P_b (hr)	e	i (deg)	δ (deg)	Φ_0 (deg)	σ_{TOA} (μs)	T (yr)	BF	References
J0737–3039A	1.38	1.24	2.45	0.08	89.3	< 3.2	45.0^{a}	10.0	26.7	1.0	[15]
J1537+1155 ^b	1.33	1.34	10.0	0.27	77.7	27^{+3}_{-3}	290^{+20}_{-20}	5.0	39.2	1.0	[17, 18]
J1757–1854	1.34	1.39	4.40	0.60	85.3	$55.60^{+1.88}_{-2.01}$	$169.40^{+1.80}_{-2.21}$	10.0	15.1	14.3	[19]
J1915+1606 ^c	1.43	1.39	7.75	0.61	132.8	22^{+3}_{-8}	55^{+5}_{-5}	8.0	49.0	2.3	[12, 20]
J1946+2052	1.23	1.24	1.88	0.06	63.0	$0.21^{+0.21}_{-0.10}$	$138.18^{+17.39}_{-44.25}$	9.0	15.1	1.1	[21, 22]

^a This value is arbitrarily chosen as there is no observational constraint on Φ_0 .

^b This pulsar is historically referred to as PSR B1534+12.

^c This pulsar is historically referred to as PSR B1913+16, or the “Hulse-Taylor pulsar.”

TABLE I. A selection of orbital parameters for five compact DNS pulsars that have constraints or significant measurements of (δ, Φ_0) from confirmed geodetic precession. Reported statistical uncertainties reflect 68.3% credibility intervals. Values with no listed uncertainties have reported precision at scales smaller than the significant digits listed in this table.

dependent measurements of δ obtained through pulse-structure analyses. Moreover, a similarly small fraction of DNS systems exhibit consistent timing precision at the $O(10 \mu\text{s})$ level or better. We therefore restricted an analysis of the known pulsars in DNS systems to five sources: PSR J0737–3039A; J1537+1155; J1757–1854; J1915+1606; and J1946+2052. A summary of existing measurements and derived quantities for these systems that are used in our simulations is provided in Table I.

For each known pulsar, we conducted a simulation similar to that first described in §III by creating arrival-time data sets containing the expected signature of $\dot{\omega}_{\text{LT},t}$. As done in §III, we limited the injected signature of LT precession to be represented only by $\dot{\omega}_{\text{LT},t}$ as $\dot{\omega}_{\text{LT},0}$ represents a constant term that contributes to the directly measured $\dot{\omega}_c$. The simulations used the latest timing solutions, and estimates of (δ, Φ_0) published in the works quoted within Table I. We also assumed that $I_p = 1.25 \times 10^{45} \text{ g cm}^2$ for all pulsars.

A key ingredient for these simulations is an accurate measure of σ_{TOA} for each pulsar. Analyses of relativistic DNS pulsars typically resolve TOAs over several-minute periods and across a number of electromagnetic frequency channels; the former procedure is important for minimizing potential smearing due to unmodeled orbital variations, while the latter is required for modeling pulse dispersion and its stochastic variation over time. However, LT precession is an achromatic timing effect, i.e., it affects all “frequency-resolved” TOAs in the same manner. Moreover, we are currently interested in constraining the presence of LT precession through pulsar timing and do not explicitly account for dispersion variations due to its stochastic nature. We therefore computed a characteristic, “frequency-averaged” value for σ_{TOA} by dividing the reported mean values of frequency-resolved TOA uncertainties by the square root of the number of frequency channels.

With these initial parameters, we then simulated a pulse-arrival-time data set with timespan T for each pulsar that begins with the earliest quoted TOA date up to the beginning of 2030. In keeping with §III, we simulated TOAs that contain only the expected signature of $\dot{\omega}_{\text{LT},t}$; we also injected random Gaussian noise such that the TOA residuals produce a reduced goodness-of-fit statis-

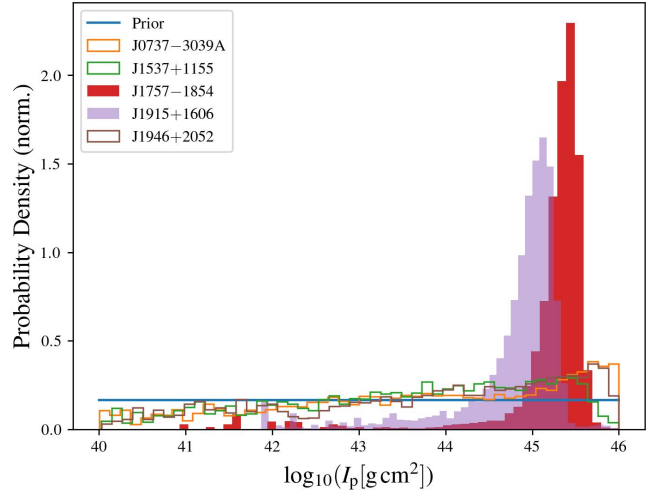


FIG. 2. Posterior distributions of I_p obtained through MCMC-based optimization of the modified DDGR model against simulated data of three known DNS pulsars that include $\dot{\omega}_{\text{LT},t}$. These data sets are generated assuming that each pulsar is observed for 20 years, and that the timing precision is consistent with published analyses. While less compact, PSR J1757–1854 is the only known source expected to exhibit a measurable $\dot{\omega}_{\text{LT},t}$ due to substantial misalignment between \mathbf{S}_p and \mathbf{L} .

tic of ~ 1 when weighted by σ_{TOA} . Finally, we used the Markov Chain Monte Carlo (MCMC) capabilities within PINT for Bayesian probabilistic sampling of timing-model parameters against the simulated TOA data sets. In order to constrain the presence of LT precession, we held (δ, Φ_0) fixed to the median values reported in Table I while assuming a log-uniform prior in I_p over six orders of magnitude; all other parameters – the five Keplerian orbital elements as well as (m_c, m_{tot}) – were sampled assuming Gaussian priors centered on their simulation values and with widths ten times greater than least-squares estimates of their statistical uncertainties.

Figure 2 presents the posterior distribution of I_p obtained from our MCMC simulations of timing-model accuracy against simulated TOAs. Three of the five pulsars listed in Table I yield posterior distributions that do not

significantly deviate from the prior distribution. Moreover, the Bayes factor (BF) of statistical evidence [23] for each of these simulations is consistent with unity, indicating that there is no meaningful evidence of a departure from the null hypothesis. It is worth noting that two of these three DNS pulsars are within the most “compact” systems given their low values of P_b ; their measurements of δ indicate low or even insignificant misalignment between \mathbf{L} and \mathbf{S}_p . This low alignment leads to $\dot{\omega}_{LT} \approx \dot{\omega}_{LT,0}$. Although PSR J1537+1155 is moderately misaligned, its lower degree of compactness corresponds to less geodetic precession and therefore primarily linear variations due to LT precession.

By contrast, the BFs of our simulations indicate that PSRs J1757–1854 and J1913+1606 will show statistically significant evidence for $\dot{\omega}_{LT,t}$ by 2030. This circumstance is arguably surprising for J1757–1854 due to T spanning only 15 years by 2030, among the lowest in Table I. Moreover, both pulsars have similar values of (σ_{TOA}, e) while the data set for J1916+1606 will span essentially five decades by the same time. However, the lower P_b for J1757–1854 leads to a higher rate of geodetic precession than in J1915+1606, such that $(\Omega_p)_{J1757} \approx 3(\Omega_p)_{J1915}$. This difference in Ω_p leads to a comparable amount of geodetic precession over the respective timespans despite the large difference in T . Furthermore, P_s for J1757–1854 is nearly three times smaller than that for J1915+1606, therefore increasing the amplitude of $\dot{\omega}_{LT}$ by a similar amount as indicated in Equations 6–7. All of these circumstances lead to a greater amount of nonlinear orbital variations from LT precession in the J1757–1854 system.

V. DISCUSSION

Our simulations demonstrate that nonlinear variations in x and ω for DNS pulsars will arise from LT precession if \mathbf{L} and \mathbf{S}_p are significantly misaligned. This nonlinearity can be detected through pulsar timing so long as several observing observational conditions are achieved – particularly obtaining sufficient timing precision, orbital geometry, and timespan – as explored in §IV. When using the parameters of known pulsars, we found that the nonlinear variation in ω due to LT precession should be detectable in PSRs J1757–1854 and J1915+1606 by 2030. Such detections allow for a constraint on I_p if (δ, Φ_0) are *a priori* known.

The simulations presented above do not account for sources of statistically “red” noise in pulsar TOA analysis. Examples of typical red noise in TOAs include stochastic variations in pulse dispersion [e.g., 24], and other sources of “timing noise” related to the instability in pulsar rotation [e.g., 25]. The presence of red noise in

pulsar TOAs represents a fundamental limit in achievable TOA precision, and therefore similarly limits the ability to test GR using DNS pulsars [e.g., 26]. However, a variety of methods exist to simultaneously model red noise through heuristic means [e.g., 27]. Moreover, red-noise processes will only limit the resolution of LT precession if left unmodeled and its magnitude exceeds the $O(10 \mu s)$ maximum amplitude of variations induced by LT precession. We therefore do not expect “typical” red noise with $O(10 \mu s)$ amplitude or lower to hinder timing-based measurements of LT precession.

An atypical source of red noise unique to DNS pulsars is the long-term change in the pulse profile induced by geodetic precession. This secular change is expected to produce variations in P_s [28]. Nearly all known DNS pulsars exhibit slowly varying profiles whose resultant timing variations can be modeled with a polynomial expansion of P_s . However, the relativistic PSR J1906+0746 shows extreme timing noise due to substantial pulse-profile evolution, with a magnitude well in excess of $O(10 \mu s)$ [29]. Such a system is therefore not suitable for pulsar-timing measurements of LT precession, though pulse-structure analyses of J1906+0746 allow for a direct measurement of geodetic precession [30].

As discussed in §IV, the detections of \dot{x}_{LT} and $\dot{\omega}_{LT,t}$ in known DNS pulsars will not be statistically strong enough to separately constrain (I_p, δ, Φ_0) from the pulsar-timing signatures alone. Independent estimates of (δ, Φ_0) through pulse-structure analyses are therefore crucial for using the detection of LT precession to constrain I_p in these known systems. Nevertheless, detections of nonlinear orbital variations from LT precession can serve other purposes when assuming an EoS and therefore a value of I_p :

- checking for self-consistency in (δ, Φ_0) inferred from pulse-structure analysis;
- testing for deviations from Equation 2 that may indicate significant spin-orbit coupling of the unobserved neutron star;
- deriving a timing-based measurement of Ω_p .

By contrast, the discovery of any “ultra-compact” DNS pulsar – with $P_b < 2$ hr – will better approximate the ideal case considered in §III and thus allow for separated measurements of (I_p, δ, Φ_0) through pulsar timing. Such systems will therefore provide the best opportunities to observe nonlinear variations from LT precession.

ACKNOWLEDGMENTS

E. F. is supported by the National Science Foundation under grant AST-2407399.

-
- [1] I. H. Stairs, Testing General Relativity with Pulsar Timing, *Living Rev. Relativ.* **6**, 5 (2003).
- [2] P. C. C. Freire and N. Wex, Gravity experiments with radio pulsars, *Liv. Rev. Rel.* **27**, 5 (2024).
- [3] F. Özel and P. C. C. Freire, Masses, Radii, and the Equation of State of Neutron Stars, *Ann. Rev. Astron. Astrop.* **54**, 401 (2016).
- [4] Pulsar timing is only sensitive to radial displacements of the pulsar, which do not depend on Ω . The rate of change in Ω due to LT precession is therefore not directly measurable and is subsequently ignored in further discussion.
- [5] H. Hu and P. C. C. Freire, Measuring the Lense–Thirring Orbital Precession and the Neutron Star Moment of Inertia with Pulsars, *Universe* **10**, 160 (2024).
- [6] In what follows, we assume that the spin of the pulsar’s companion object is negligible, i.e., $|\mathbf{S}_c| \ll |\mathbf{S}_p|$ so that $\mathbf{J} \approx \mathbf{L} + \mathbf{S}_p$. LT precession in DNS systems will therefore be dominated by the spin of the pulsar.
- [7] T. Damour and J. H. Taylor, Strong-field tests of relativistic gravity and binary pulsars, *Phys. Rev. D* **45**, 1840 (1992).
- [8] T. Damour and J. H. Taylor, On the Orbital Period Change of the Binary Pulsar PSR 1913+16, *Astrophys. J.* **366**, 501 (1991).
- [9] P. C. Peters, Gravitational Radiation and the Motion of Two Point Masses, *Phys. Rev.* **136**, 1224 (1964).
- [10] T. Damour and G. Schafer, Higher-order relativistic periastron advances and binary pulsars., *Nuo. Cim. B Ser.* **101B**, 127 (1988).
- [11] S. M. Kopeikin, Proper Motion of Binary Pulsars as a Source of Secular Variations of Orbital Parameters, *Astrophys. J. Lett.* **467**, L93 (1996).
- [12] M. Kramer, Determination of the Geometry of the PSR B1913+16 System by Geodetic Precession, *Astrophys. J.* **509**, 856 (1998).
- [13] J. M. Cordes, I. Wasserman, and M. Blaskiewicz, Polarization of the Binary Radio Pulsar 1913+16: Constraints on Geodetic Precession, *Astrophys. J.* **349**, 546 (1990).
- [14] V. Radhakrishnan and D. J. Cooke, Magnetic Poles and the Polarization Structure of Pulsar Radiation, *Astrophys. Lett.* **3**, 225 (1969).
- [15] M. Kramer, I. H. Stairs, R. N. Manchester, N. Wex, A. T. Deller, W. A. Coles, M. Ali, M. Burgay, F. Camilo, I. Cognard, T. Damour, G. Desvignes, R. D. Ferdman, P. C. C. Freire, S. Grondin, L. Guillemot, G. B. Hobbs, G. Janssen, R. Karuppusamy, D. R. Lorimer, A. G. Lyne, J. W. McKee, M. McLaughlin, L. E. Münch, B. B. P. Perera, N. Pol, A. Possenti, J. Sarkissian, B. W. Stappers, and G. Theureau, Strong-Field Gravity Tests with the Double Pulsar, *Phys. Rev. X* **11**, 041050 (2021).
- [16] J. Luo, S. Ransom, P. Demorest, P. S. Ray, A. Archibald, M. Kerr, R. J. Jennings, M. Bachetti, R. van Haasteren, C. A. Champagne, J. Colen, C. Phillips, J. Zimmerman, K. Stovall, M. T. Lam, and F. A. Jenet, PINT: A Modern Software Package for Pulsar Timing, *Astrophys. J.* **911**, 45 (2021).
- [17] I. H. Stairs, S. E. Thorsett, and Z. Arzoumanian, Measurement of Gravitational Spin-Orbit Coupling in a Binary-Pulsar System, *Phys. Rev. Lett.* **93**, 141101 (2004).
- [18] E. Fonseca, I. H. Stairs, and S. E. Thorsett, A Comprehensive Study of Relativistic Gravity Using PSR B1534+12, *Astrophys. J.* **787**, 82 (2014).
- [19] A. D. Cameron, M. Bailes, D. J. Champion, P. C. C. Freire, M. Kramer, M. A. McLaughlin, C. Ng, A. Possenti, A. Ridolfi, T. M. Tauris, H. M. Wahl, and N. Wex, New constraints on the kinematic, relativistic, and evolutionary properties of the PSR J1757-1854 double neutron star system, *Mon. Not. Roy. Astron. Soc.* **523**, 5064 (2023).
- [20] J. M. Weisberg and Y. Huang, Relativistic Measurements from Timing the Binary Pulsar PSR B1913+16, *Astrophys. J.* **829**, 55 (2016).
- [21] L. Meng, W. Zhu, M. Kramer, X. Miao, G. Desvignes, L. Shao, H. Hu, P. C. C. Freire, Y. Zhang, M. Xue, Z. Fang, D. J. Champion, M. Yuan, C. Miao, J. Niu, Q. Fu, J. Yao, Y. Guo, and C. Zhang, The Relativistic Spin Precession in the Compact Double Neutron Star System PSR J1946+2052, *Astrophys. J.* **966**, 46 (2024).
- [22] L. Meng, P. C. C. Freire, K. Stovall, N. Wex, X. Miao, W. Zhu, M. Kramer, J. M. Cordes, H. Hu, J. Jiang, E. Parent, L. Shao, I. H. Stairs, M. Xue, A. Brazier, F. Camilo, D. J. Champion, S. Chatterjee, F. Crawford, Z. Fang, Q. Fu, Y. Guo, J. W. T. Hessels, M. MacLaughlin, C. Miao, J. Niu, Z. Wu, J. Yao, M. Yuan, Y. Yue, and C. Zhang, The double neutron star PSR J1946+2052 I. Masses and tests of general relativity, *arXiv e-prints*, arXiv:2510.12506 (2025).
- [23] For each simulation, we compute the BF using the Savage-Dickey ratio of the prior and posterior distributions evaluated at $\log_{10} I_p = 43$.
- [24] M. L. Jones, M. A. McLaughlin, M. T. Lam, J. M. Cordes, L. Levin, S. Chatterjee, Z. Arzoumanian, K. Crowter, P. B. Demorest, T. Dolch, J. A. Ellis, R. D. Ferdman, E. Fonseca, M. E. Gonzalez, G. Jones, T. J. W. Lazio, D. J. Nice, T. T. Pennucci, S. M. Ransom, D. R. Stinebring, I. H. Stairs, K. Stovall, J. K. Swiggum, and W. W. Zhu, The NANOGrav Nine-year Data Set: Measurement and Analysis of Variations in Dispersion Measures, *Astrophys. J.* **841**, 125 (2017).
- [25] M. Antonelli, A. Basu, and B. Haskell, Stochastic processes for pulsar timing noise: fluctuations in the internal and external torques, *Mon. Not. Roy. Astron. Soc.* **520**, 2813 (2023).
- [26] H. Hu, Unlocking gravity and gravitational waves with radio pulsars: advances and challenges, *Astrophys. Spa. Sci.* **370**, 74 (2025).
- [27] D. J. Reardon, A. Zic, R. M. Shannon, V. Di Marco, G. B. Hobbs, A. Kapur, M. E. Lower, R. Mandow, H. Middleton, M. T. Miles, A. F. Rogers, J. Askew, M. Bailes, N. D. R. Bhat, A. Cameron, M. Kerr, A. Kulkarni, R. N. Manchester, R. S. Nathan, C. J. Russell, S. Osłowski, and X.-J. Zhu, The Gravitational-wave Background Null Hypothesis: Characterizing Noise in Millisecond Pulsar Arrival Times with the Parkes Pulsar Timing Array, *Astrophys. J. Lett.* **951**, L7 (2023).
- [28] M. Konacki, A. Wolszczan, and I. H. Stairs, Geodetic Precession and Timing of the Relativistic Binary Pulsars PSR B1534+12 and PSR B1913+16, *Astrophys. J.* **589**, 495 (2003).
- [29] J. van Leeuwen, L. Kasian, I. H. Stairs, D. R. Lorimer, F. Camilo, S. Chatterjee, I. Cognard, G. Desvignes,

- P. C. C. Freire, G. H. Janssen, M. Kramer, A. G. Lyne, D. J. Nice, S. M. Ransom, B. W. Stappers, and J. M. Weisberg, The Binary Companion of Young, Relativistic Pulsar J1906+0746, *Astrophys. J.* **798**, 118 (2015).
- [30] G. Desvignes, M. Kramer, K. Lee, J. van Leeuwen, I. Stairs, A. Jessner, I. Cognard, L. Kasian, A. Lyne, and B. W. Stappers, Radio emission from a pulsar's magnetic pole revealed by general relativity, *Science* **365**, 1013 (2019).